Journal of Modern Researches on Electronic Defense Systems

Receive: 20 June 2024 Accept: 3 November 2024

A Novel High-Gain Fractal Antenna Array with Metamaterial as Superstrate for Electronic Defense Systems

Farzad Mohajeri[1*], Ali Emamghorashi

[*]Corresponding Author: mohajeri@shirazu.ac.ir

[1]Department of Communications and Electronics, School of Electrical and Computer Engineering, Shiraz University, Shiraz, Iran.

[2] Department of Electrical Engineering, Islamic Azad University, Fasa Branch, Fasa, Iran.

Abstract – *In this paper, a near zero-index metamaterial (NZIM) unit cell, for gain improvement of a two-element antenna array is proposed, designed, and fabricated. The near-zero refractive index characteristics of metamaterial superstrate are used, which gathers the radiated waves from the source antenna and collimates them toward the normal direction. The array elements are formed by constructing a dual triangle Koch fractal (DTKF) to the periphery of a square patch, to benefit miniaturization and mutual coupling reduction properties of fractals. Fractal geometry leads to a 300MHz reduction in resonance frequency of the unloaded antenna array, which means an acceptable miniaturization. A prototype of this antenna has been fabricated and measured. Measured results are in good agreement with the simulation. The simulated and measured results have shown a gain enhancement at the corresponding resonance frequency of the antenna array. It is seen that at 3.15 GHz, where the refractive index is near its minimum value, the simulated broadside gain is 2 dB higher than that of an unloaded antenna array. The NZIM antenna also exhibits an HPBW reduction of about* 20^0 *and* 14^0 *in the E plane and H plane, respectively.*

Keywords: *Koch fractal antenna, Near-zero index metamaterial, Antenna array, Gain, HPBW.*

1. Introduction

Modern wireless communication systems require a low profile, light weight, high gain, and simple structure antennas to assure reliability, mobility, and high-efficiency characteristics. Microstrip antennas generally meet the requirements of a high level of compactness, low cost, and ease of fabrication as their benchmarks. On the other side of the coin, they suffer from a few demerits, like low gain and narrow bandwidth [1]. So, many studies have been published on the performance improvement of patch antennas among them, gain enhancement and miniaturization are of special interest.

The low gain problem of a single microstrip patch antenna can be further improved by different techniques. One commonly used method is, for example, using a high permittivity substrate. However, surface wave excitation lowers radiation efficiency and pattern degradation, which are the main drawbacks of this method. So, researchers focus mostly on two other major gain-enhancing techniques. The first uses an array antenna configuration with a proper feeding network [2], whereas the second adopts newly developed materials called metamaterials [3]. In recent years, combining these two methods has paved a new way for designing novel high-gain microstrip antennas.

In recent years, the increasing progress of technology has caused the need for compression in designs, which makes it possible to integrate devices with other components. So, fractal geometry is incorporated in the array antenna design to accomplish the anticipated miniaturization and reduce mutual coupling. It is shown that using the fractal configuration in linear array antenna design would result in denser packing while minimizing mutual coupling [4-6].

In recent times, the development of metamaterials has opened a new possibility for designers to overcome some mentioned problems. Different types of superstrate and substrate metamaterials have been proposed to obtain gain enhancement of microstrip array antennas, including electromagnetic band gap structures (EBGs) [7], artificial magnetic conductors (AMC) [8], and frequency selective surfaces (FSS) [9]. A double-element microstrip antenna array inserted with an EBG structure has been investigated in [7]. It has been provided that using EBG is a convenient way to 1 dBi increase the array gain. In [8], a 4-element array with AMC is proposed. The simulated and measured results

demonstrate significant improvements. The loaded AMC array achieves 15.9 dBi gain compared to 13 dBi gain without AMC. In [9], Farooq Sultan and his collegiate team succeeded in getting a directivity boost of 3 dBi that is achieved by using FSS as a superstrate of the antenna array. Among different kinds of metamaterials, near zero-index metamaterial (NZIM), is of special interest. NZIM can collimate the diverging waves into plane waves. This collimation property increases the directivity and gain of the antenna [10]. So, it is worth combining the concept of fractal structures with the linear antenna array, while using the benefits of NZIM configurations.

In this article, a narrowband fractal patch antenna with NZIM as a superstrate is investigated. The aim of this work is the gain enhancement in the operating frequency of the antenna array. Simulation results obtained by the HFSS show a noticeable increase in the directivity of the NZIM antenna array compared to a simple patch without NZIM. The proposed antenna was also fabricated and its performance was demonstrated through measurement. Thus, the authors have extended the application of NZIM loading to the array of fractal microstrip patch antennas for gain enhancement.

The structure of this paper is as follows. In section 2, different parts of the antenna array are discussed. First of all, the basic element that forms an array is introduced. The construction of the array and its feeding network are analyzed. At last, the NZIM superstrate layer is introduced. Section 3, combines the antenna array with the NZIM superstrate layer, where the whole array structure is formed. In section 4, fabrication and measurement results are investigated and compared.

2.Analysis and Design of Antenna Array Elements

2.1 Single Element Fractal Patch Antenna

To investigate the characteristics of a fractal patch, the schematic of the simple square patch with the construction of a dual triangle Koch fractal (DTKF) to the periphery of that square patch is shown in Fig.1. Rogers 4003 substrate is selected with dielectric constant $\varepsilon_r = 3.55$, loss tangent $tan\delta_c = 0.0027$, and height= 1.6 mm. Dimensions of simple square patch is selected so that, the resonance frequency of the antenna is set to 3 GHz. The patch is a 33×25 mm^2 metal rectangle on the dielectric substrate with Wsub=66 mm, Lsub=50 mm. The Ansis HFSS full-wave software is used for all computer simulations and the data obtained in this paper. It is shown that the increase of the side length of an equilateral triangle e.g., a, leads to the decrease of the resonance frequency of the antenna. Table 1, shows a decrease of resonance frequency without the deterioration of gain, as the side length of the equilateral triangle varies from 2 mm to 6 mm. Thus, miniaturization of the antenna is effectively obtained [11].

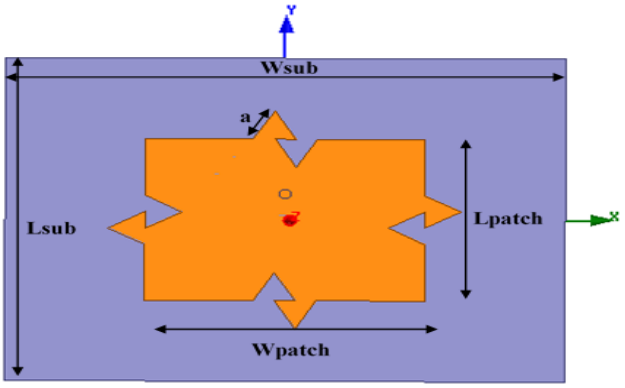

Figure 1. DTKF first iteration (top view)

Table 1. Effect of varying the fractal dimension on the antenna parameters

Side length a (mm)	Resonance Frequency (GHz)	Bandwidth (MHz)	Fractional Bandwidth %	Gain (dB)
2	2.97	47	1.59	6.9
3	2.93	47	1.58	7
4	2.87	43	1.48	7
5	2.77	39	1.43	6.9
6	2.68	34	1.3	6.7
rectangle	3.01	65	2.1	7

2.2 Single Element Fractal Patch Antenna

The configuration of the proposed fractal patch antenna array is presented in this section. Fig. 2, depicts the geometrical structure of a two-element antenna array, which has been constructed on a Rogers4003 substrate dielectric with a height of 1.6 mm, and dimensions of $100 \times 100\ mm^2$ by a 50 Ω coaxial cable. The side length of the equilateral triangle of the fractal patch (a) and the inset feed y_0 to match the 50 Ω input impedance of each fractal patch to the microstrip line feed, are set at 5 mm and 9.4 mm, respectively.

The feeding network is designed in such a way, that the input power is equally divided between two sections of array elements. Fig. 3, shows the feeding network schematic of the antenna array with the associated parameters. The width and length of all sections of the feeding network are designed, using power divider equations of microstrip lines [12]. The first section is a 50 Ω microstrip line with W1=3.57 mm to match the 50 Ω coaxial cable. Two equally 100 Ω parts form the second section of the feeding network with a width of W2= 0.9 mm. In the last section, a $\lambda_g/4$ impedance transformer is used, to match a 100 Ω to 50 Ω line, where λ_g represents the guided wavelength. The total width and length of this section are 1.95 mm and 13.92 mm, respectively. To have a better understanding of the proposed antenna array, the simulated return loss parameter of the unloaded antenna

array (array antenna without NZIM superstrate) is shown in Fig. 4. It is seen that the resonance frequency of the proposed array is around 2.88 GHz, which is 300 MHz less than the corresponding antenna array with simple rectangle patch. So, the miniaturization is obtained effectively. The gain radiation pattern of the antenna array at the resonance frequency of 2.88 GHz in both E and H planes is shown in Fig. 5. These patterns, show a broadside behaviour in antenna radiation and also reach the maximum broadside gain of 9 dBi, which is about 2 dBi higher than that of a simple microstrip patch antenna. The calculated half power beam widths (HPBW) in both E and H planes are 74^0 and 54^0, respectively.

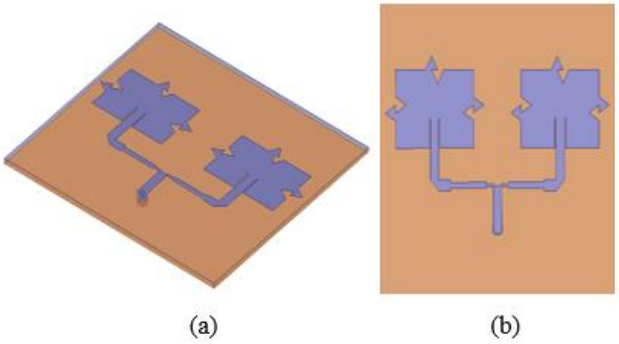

Figure 2. Geometrical structure of a two-element fractal antenna array (a) 3D view, (b) top view

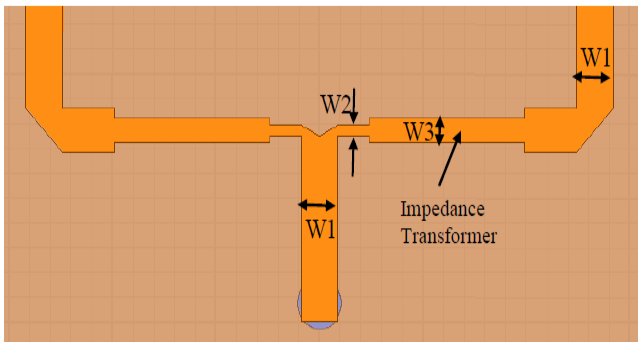

Figure 3. Top view schematic of feeding network of two-element antenna array

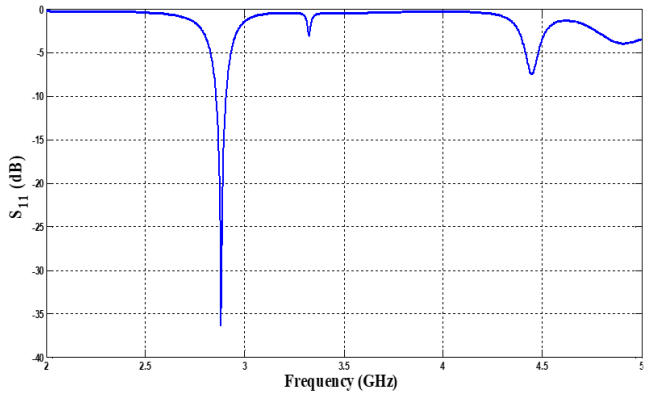

Figure 4. The simulated S_{11} parameter of the unloaded antenna array

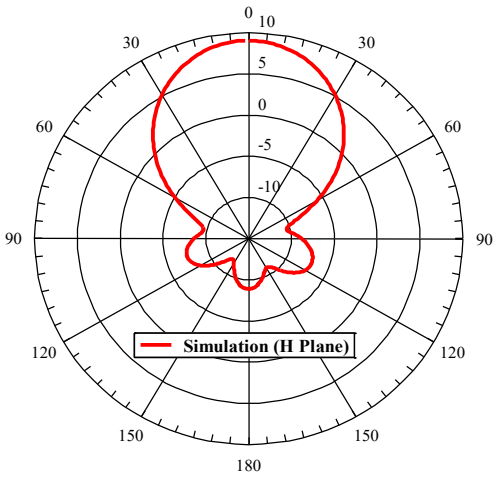

(a)

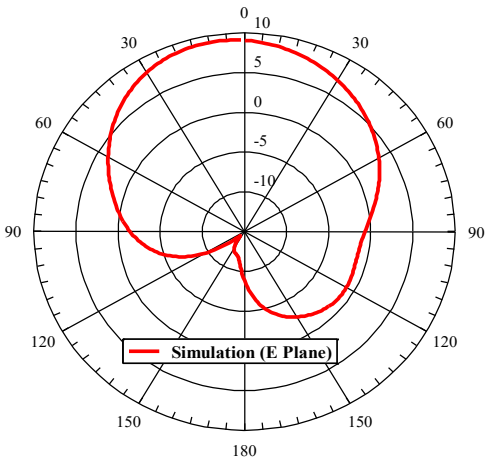

(b)

Figure 5. The simulated radiation patterns of the unloaded antenna array at 2.88 GHz (a) H-Plane, (b) E-Plane

2.3 Metamaterial Unit Cell

In this section, metamaterial unit cell geometry is introduced. The array arrangement of these unit cells forms the NZIM metamaterial. The schematic configuration of the proposed metamaterial unit cell is shown in Fig. 6 [13]. The unit cell consists of a set of metallic strips printed on both sides of a substrate. Rogers 4003 substrate is selected with a dielectric constant of 3.55, loss tangent $tan\delta_c = 0.0027$, and height, h=1.6 mm. The periodicity is denoted by $p_x = 10\ mm$ and $p_y = 10\ mm$ in x and y directions, respectively. A set of design parameters, such as the width and length of metal lines, as depicted in Fig. 6, define the geometry of the unit cell. These parameters allow us to design a metamaterial with an effective refractive index of less than one in the desired frequency range. The values of geometry parameters obtained from the optimization procedure for the unit cell are summarized in Table 2 [13].

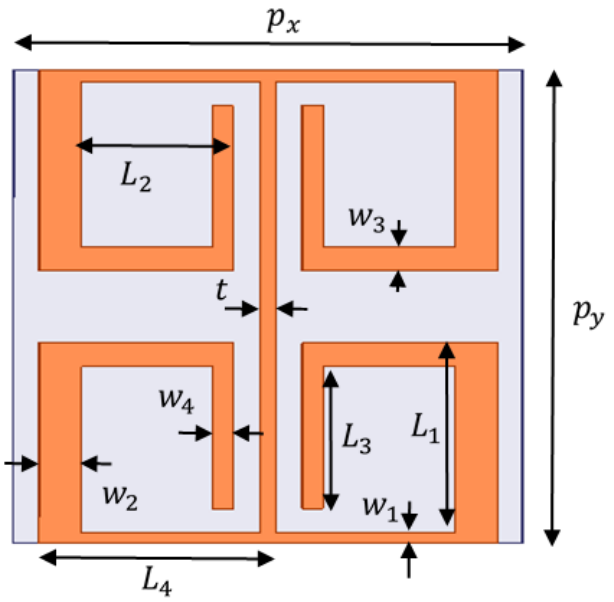

Figure 6. Top view configuration of the proposed metamaterial unit cell

Table 2. Optimized parameters of the proposed metamaterial unit cell in mm

L_1	L_2	L_3	L_4	w_1	w_2	w_3	w_4	t
4	3.02	3	4.51	0.24	0.82	0.52	0.41	0.32

3. Proposed Loaded Antenna Array with NZIM Superstrate

In this section, the new unit cell presented in the previous section is employed to design the whole structure of the antenna array. So, our designed high-gain antenna array is formed by a two-element microstrip fractal patch antenna as a radiation source, on which a two-layer NZIM is superposed, as shown in Fig. 7. The superstrate consists of two layers, each layer having an array of 9 × 9-unit cells in both x and y directions. The parametric sweep in HFSS, reveals that the best distance from the radiation source and the bottom of the first layer should be selected about 7 mm. At this distance, the maximum gain is obtained without degrading the radiation pattern considerably. The variations of return loss versus frequency of the loaded antenna array are shown in Fig. 8. It is seen that the resonance frequency of the loaded antenna array, shifts to about 3.15 GHz, where $|S_{11}|$ is -17 dB. This is the frequency in which the effective refractive index of NZIM superstrate reaches its minimum, e.g., near zero.

The radiation patterns of the loaded antenna array at the resonance frequency of 3.15 GHz are also illustrated in Fig. 9. As shown, it is obvious that the NZIM superstrate layer leads to a narrower radiation pattern and more gain enhancement of the whole structure. It is worth mentioning that, despite the NZIM layer, the radiation pattern preserves its broadside characterization, and no distortion is observed. The calculated half-power beam widths (HPBW) in both E and H planes are 54^0 and 40^0, respectively.

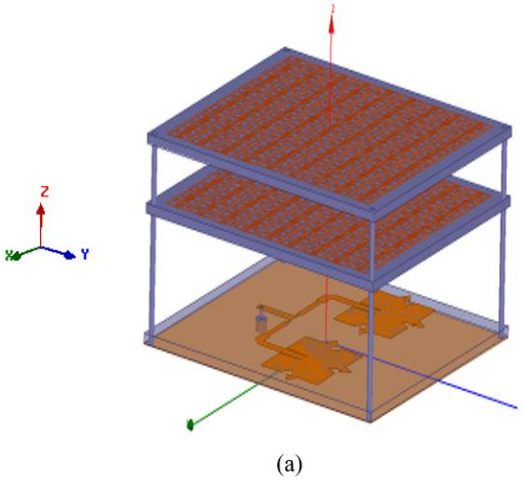

(a)

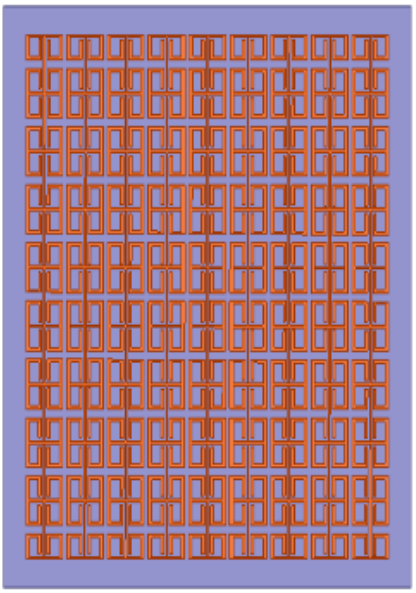

(b)

Figure 7. (a) 3D view of the loaded antenna array (b) top view of NZIM layer

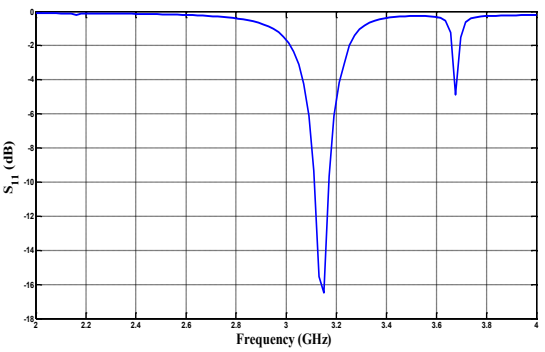

Figure 8. The simulated return loss parameter of the loaded antenna array

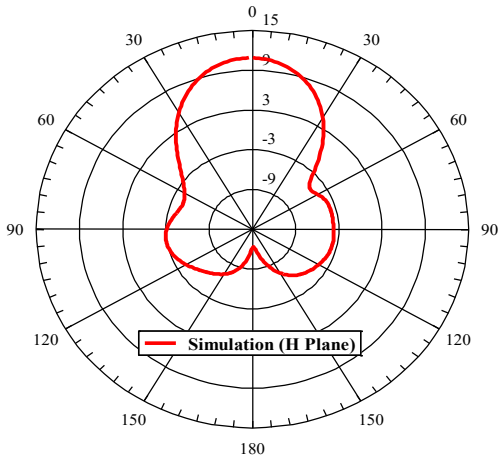

(a)

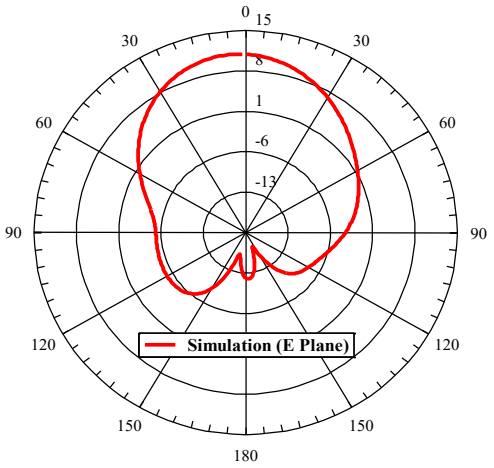

(b)

Figure 9. The simulated radiation patterns of the loaded antenna array at 3.15 GHz (a) H-Plane, (b) E-Plane

The comparison between the co and cross-polarization for loaded and unloaded antenna array in the resonant frequencies are shown in Figs. 10 and 11 in both E and H planes. In these figures, cross-polarization is less than co-polarization, significantly. Gain variations of the loaded and unloaded antenna array versus frequency are compared in Fig. 12. The effect of the NZIM layer in gain enhancement is seen apparently in a wide frequency range, where the effective refractive index or N_{eff} decreases below 0.5. As the N_{eff} approaches zero, the effect of the gain increase is more obvious. At the resonance frequency of 3.15 GHz, where N_{eff} is near its minimum, the gain reaches 11 dBi, 2 dBi higher than the unloaded antenna at its corresponding resonance frequency. At last, Table 3, compares different parameters of the loaded and unloaded antenna array.

4. Simulation and Measurement Results

The proposed antenna array has been fabricated and meas ured to show the validity of the designed and simulated resu lts and then the simulated and measured results are compare d. The fabricated patch antenna with optimized NZIM super strate is shown in Fig. 13.

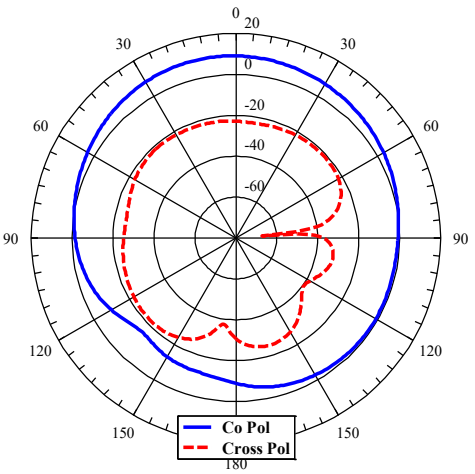

(a)

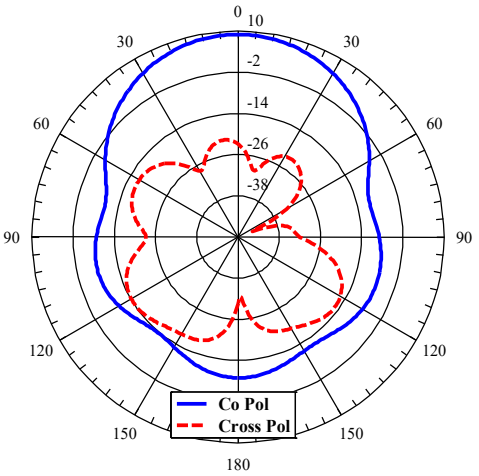

(b)

Figure 10. The simulated co and cross-polarization radiation patterns of the unloaded antenna array at 2.88 GHz (a) E-Plane, (b) H-Plane

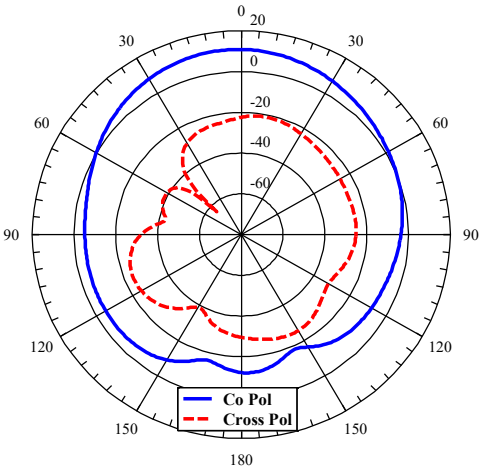

(a)

The simulated and measured return loss of the loaded antenna array is shown in Fig. 14. It is observed that both

results are in good agreement with each other, confirming the validity of the design. Fig. 15 shows the simulated and measured elevation plane radiation pattern characteristics of the loaded antenna array, in both H-plane and E-plane, respectively.

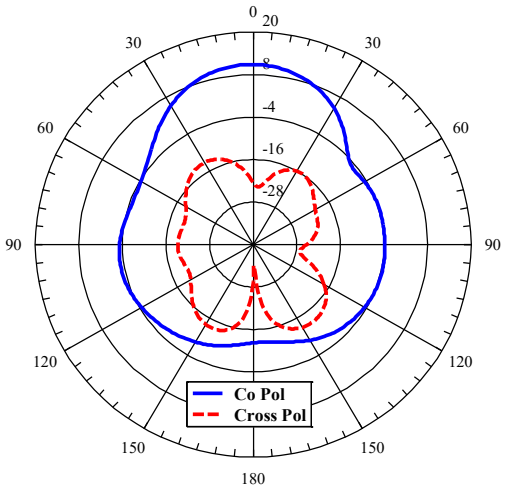

(b)

Figure 11. The simulated co and cross-polarization radiation patterns of the loaded antenna array at 3.15 GHz (a) E-Plane, (b) H-Plane

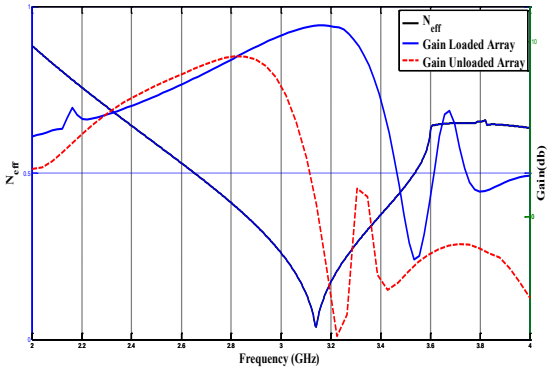

Figure 12. The comparison of gain variations of unloaded and loaded antenna array and effective refractive index versus frequency

Table 3. Comparison of different parameters of the loaded and unloaded antenna array

Antenna array parameters	Resonance Frequency (GHz)	Bandwidth (MHz)	Fractional Bandwidth (%)	Gain (dB)
Unloaded	2.88	50	1.8	9
Loaded	3.15	60	2	11

Antenna array parameters	HPBW (deg)		Co pol level (Cross pol) in dB	
	H-plane	E-plane	H plane	E plane
Unloaded	54	74	9 (-23.2)	9 (-22.9)
Loaded	40	54	10.89(-23.7)	10.85(-22.2)

The measured and simulated gain variations versus frequency are shown in Fig. 16. The closeness of both curves proves the validity of the design.

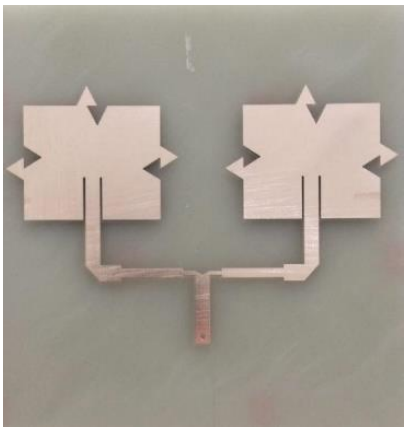

(a)

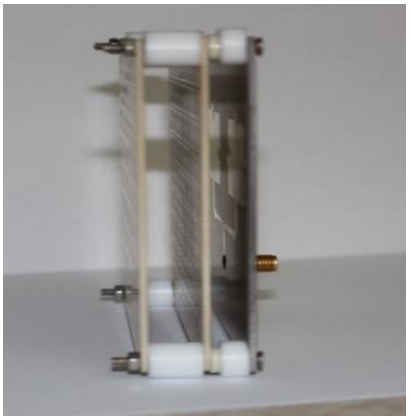

(b)

Figure 13. Fabricated antenna array (a) top view of the unloaded array (b) 3D view of the loaded array

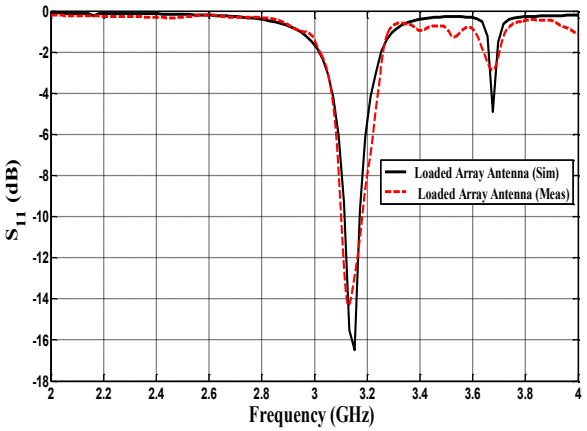

Figure 14. The simulated and measured return loss of the loaded antenna array

The comparison of the proposed loaded antenna with other recent references is specified in Table 4. As it is depicted in this table the proposed array antenna has a good gain at the appropriate bandwidth.

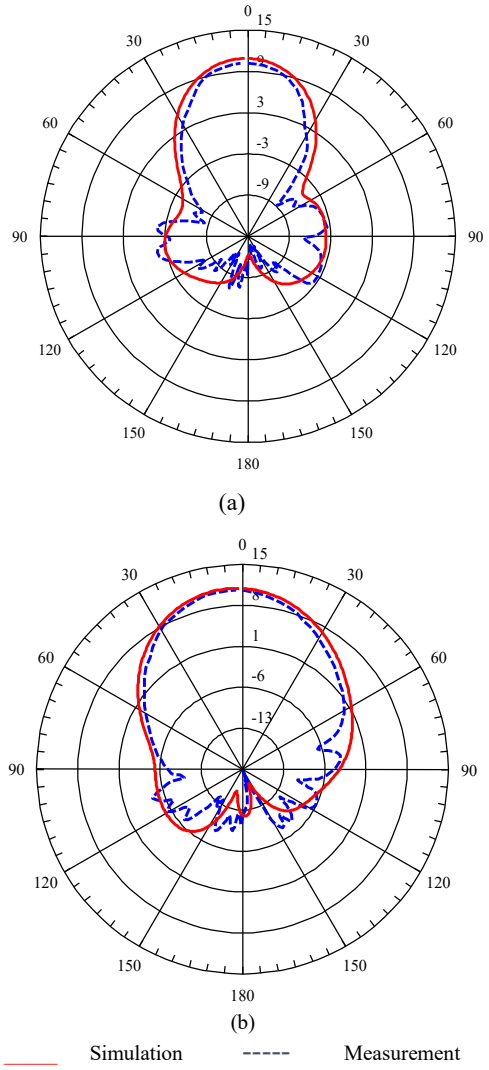

Figure 15. The simulated and measured radiation patterns of the loaded antenna array (a) H-Plane, (b) E-Plane

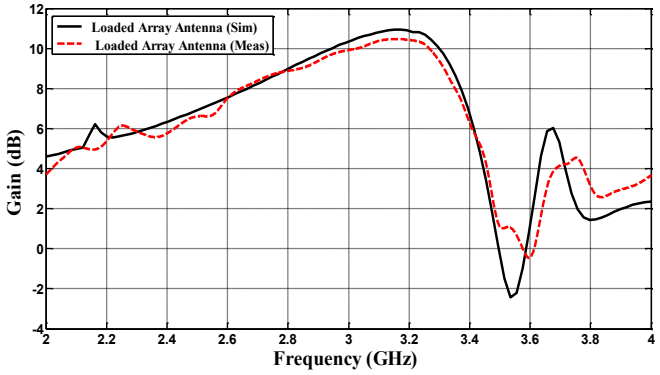

Figure 16. The simulated and measured gain variation of the loaded antenna array

Table 4. Comparison of the proposed loaded antenna with other recent references

	[4]	[5]	[6]	[11]	[13]	Proposed
Fractional Bandwidth (%)	3.4	11.4	5	1.43	31	2
Aperture Efficiency (%)	78	30.4	46	73	86	89
Max. Gain (dB)	7.2	11.3	10.66	8.6	9	11
Superstrate	2-Layer	2-Layer	1-Layer	1-Layer	2-Layer	2-Layer
Resonant Frequency (GHz)	8.75	9.9	3.57	2.77	3.7	3.15

5. Conclusion

In this work, a high-gain two-element antenna array with a planar NZIM superstrate is investigated. The array elements are formed by constructing a dual triangle Koch fractal (DTKF) to the periphery of a square patch, to benefit miniaturization and mutual coupling reduction properties of fractals. Fractal geometry leads to a 300MHz reduction in resonance frequency of the unloaded antenna array, which means an acceptable miniaturization.

The NZIM is basically designed using an RLC resonator and presents a refractive index close to zero over the operating frequency band of the antenna. NZIM superstrate focuses on the radiation beam and thereby enhances the antenna gain.

Antenna performance is studied with simulation and measurement. The proposed antenna array is fabricated and measured to support the simulated results. The simulated and measured results have shown a gain enhancement at the corresponding resonance frequency of the antenna array. It is shown that as the refractive index approaches zero, the gain increases more, compared to the unloaded antenna array.

It is seen that at 3.15 GHz, where the refractive index is near its minimum value, the simulated broadside gain is 2 dB higher than that of an unloaded antenna array. The NZIM antenna also exhibits an HPBW reduction of about 20^0 and 14^0 in the E and H planes, respectively.

6. References

[1] C. A. Balanis, Antenna Theory: Analysis and Design. 4th ed., John Wiley and Sons, Inc, 2001.

[2] E. Levine, G. Malamud, S. Shtrikman, and D. Treves, "A study of microstrip array antennas with the feed network," IEEE Transactions on Antennas and Propagation, vol. 4, no. 37, pp. 426-434, April 1999.

[3] Y. Nilbargi, "Design and simulation of metamaterial resonator to improve bandwidth," Journal of Modern Researches on Electronics Defence Systems, vol. 2, no. 2, pp. 1-8, June 2023.

[4] H. Zhou, S. Qu, Z. Pei, Y. Yang, J. Zhang, J. Wang, and H. Ma, "A high directive patch antenna based on all-dielectric near zero-index metamaterial superstrate," Journal of Electromagnetic Waves and Applications, vol. 24, pp. 1387-1396, 2012.

[5] L. Yahong, G. Xiaojing, G. Shuai, and Z. Xiaopeng, "Zero index metamaterial for designing high-gain patch antenna,"

International Journal of Antennas and Propagation, vol. 2013, pp. 1-12, 2013.

[6] W. Ji-Jun, L. L. Gong, Y. X. Sun, Z. P. Zhu, and Y. R. Zhang, "High-gain composite microstrip patch antenna with the near-zero-refractive-index metamaterial," International Journal for Light and Electron Optics, vol. 125, no. 21, pp. 6491-6495, 2014.

[7] A. Yu and X. Zhang, "A novel method to improve the performance of microstrip antenna arrays using a dumbell EBG structure," IEEE Antennas and Wireless Propagation Letters, vol. 2, pp. 170-172, 2003.

[8] W. Yang, H. Wang, W. Che, and J. Wang, "A wideband and high-gain edge-fed patch antenna and array using artificial magnetic conductor structures," IEEE Antennas and Wireless Propagation Letters, vol. 12, pp. 769-772, June 2013.

[9] F. Sultan, R. Hussain, and S. S. Iqbal, "Design of a reduced size 7-Patch antenna array with FSS based directivity enhancement," in Proceedings of 2013 IEEE International Symposium on Phased Array Systems and Technology, MA, USA, October 2013, pp. 125-130.

[10] R. W. Ziolkowski, "Propagation in and scattering from a matched metamaterial having a zero index of refraction," Physical Review E, vol. 70, pp. 1-12, October 2004.

[11] A. Emamghorashi and F. Mohajeri, "Impedance bandwidth enhancement of a novel fabricated fractal patch antenna using invasive weed optimization algorithm," Iranian Journal of Science and Technology, Transactions of Electrical Engineering, vol. 41, no. 3, pp. 205-217, September 2017.

[12] D. M. Pozar, "Microwave Engineering," 4th ed., John Wiley and Sons, Inc, USA, 2005.

[13] A. Emamghorashi and F. Mohajeri, "An optimized wideband high directive microstrip fractal patch antenna based on near-zero-index metamaterial superstrate," Electromagnetics, vol. 37, no. 7, pp. 423-438, November 2017.